Charge Dynamics Near the Electron-Correlation Induced Metal-Insulator Transition in Pyrochlore-Type Molybdates

I. Kézsmárki,[1] N. Hanasaki,[1] D. Hashimoto,[1] S. Iguchi,[1] Y. Taguchi,[2] S. Miyasaka,[1] and Y. Tokura[1,3]

[1]*Department of Applied Physics, University of Tokyo, Tokyo 113-8656, Japan*

[2]*Institute for Materials Research, Tohoku University, Sendai 980-8577, Japan*

[3]*Spin Superstructure Project, ERATO, Japan Science and Technology Agency (JST), Tsukuba 305-8562, Japan*

(Received 2 August 2004; published 20 December 2004)

The systematics of the bandwidth controlled metal-insulator transition (MIT) are investigated for $R_2Mo_2O_7$ (R = Nd, Sm, Gd, Dy, and Ho) by measurements of dc and optical conductivity. The substantial role of electron correlation in driving the MIT is verified. With changing the R ionic radius (r) or equivalently the one-electron bandwidth, the $T = 0$ K MIT occurs at $r_c \approx r(R = \mathrm{Gd})$. The $T = 0$ K gap continuously vanishes as $\Delta \propto (r_c - r)$, while at the metallic side the decrease of Drude weight is followed towards r_c. A high-temperature incoherent state is approached through crossover regions both from the metallic and the insulating state.

DOI: 10.1103/PhysRevLett.93.266401 PACS numbers: 71.30.+h, 71.27.+a, 78.20.–e

The effect of strong electron-electron interaction, which leads to a tendency towards the formation of various ground states with broken symmetry, has been a central problem of condensed matter physics during the last few decades. Ordering of the different degrees of freedom (spin, charge, and/or orbital) usually materializes through the localization of the electronic states; therefore, the mechanism of the metal-insulator transition (MIT) has been extensively studied and a coherent picture is being developed [1,2]. The experimental efforts for the electron-correlation-driven MIT have been focused mainly on $3d$-electron systems so far. However, $4d$-electron systems with relatively wider bandwidth have also become a hot spot of the current research [3]. Among them, Mo oxides with pyrochlore structure, $R_2Mo_2O_7$, can provide a unique arena to address this question, as they undergo a MIT by changing the rare-earth component R [4–8]. Both magnetic and transport properties arise from the behavior of the electrons populating the t_{2g} subspace of Mo $4d$ levels as it was pointed out by photoemission experiments and band calculations [9]. Recently, Solovyev [10] applied a Hartree-Fock approach, using the results of local-density approximation (LDA) as a starting point and considering both on-site Coulomb and spin-orbit interaction for the Mo $4d$ electrons. The trigonal distortion splits t_{2g} levels to a higher-lying $e(t_{2g})$ doublet and to an a_{1g} state. These bands overlap on the level of LDA, but again can be separated by the Coulomb interaction. As even a more remarkable effect of U, a charge gap opens in $e(t_{2g})$. Consequently, there is a localized electron at a_{1g} level, while the other electron in the $e(t_{2g})$ state can be either localized or itinerant depending on the relative strength of the electron correlation. The interaction between the neighboring Mo spins is antiferromagnetic (AF) for a_{1g} and ferromagnetic (FM) for $e(t_{2g})$ electrons, due to superexchange and double exchange mechanism. According to their balance, the formation of FM and spin glass (SG) phases is observed on the frustrated pyrochlore lattice [4,5].

We have measured the dc resistivity (ρ) of five compounds from the $R_2Mo_2O_7$ family (R = Nd, Sm, Gd, Dy, and Ho) and observed a MIT as a function of the rare-earth radius, r. All of them were high quality single crystals grown by a floating-zone method (for details, see Ref. [7]). As previously reported [4,5], $Gd_2Mo_2O_7$ is the closest to the FM-SG phase boundary at the FM side. However, the T_c values obtained by various groups range between 35–65 K. The present study demonstrates that $Gd_2Mo_2O_7$ is located on the verge of the MIT as well, but in contrast to previous results mostly obtained on polycrystals, it is an insulator at the ground state. Because of the proximity to

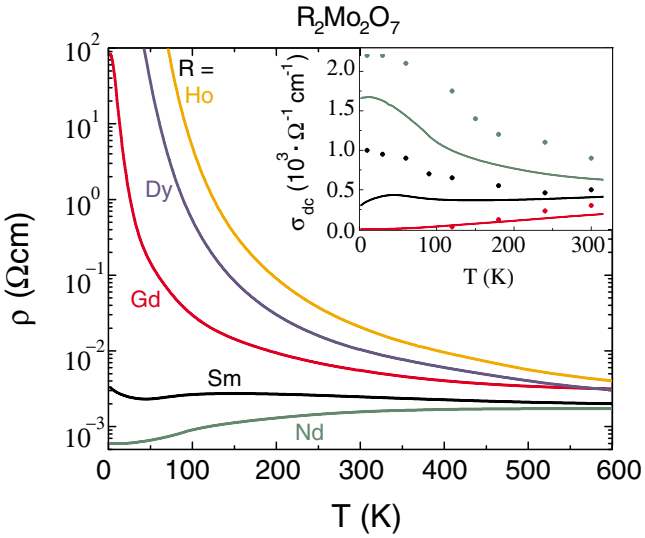

FIG. 1 (color). Temperature dependence of the resistivity for five single crystals of $R_2Mo_2O_7$. The inset shows the comparison of σ_{dc} and $\sigma(\omega \rightarrow 0)$ below $T = 300$ K for R = Gd, Sm, and Nd.

the metallic phase, its properties are extremely sensitive to the preparation and the system turn to be metallic by a small amount of hole doping [11]. $Ho_2Mo_2O_7$, $Dy_2Mo_2O_7$, and $Gd_2Mo_2O_7$ are insulators with decreasing charge gap in this order as reflected in the $\rho(T)$ curves of Fig. 1. $Sm_2Mo_2O_7$ and $Nd_2Mo_2O_7$ show the characteristics of bad metals. Except for the low-temperature phase of $Nd_2Mo_2O_7$, their resistivity is above the Ioffe-Regel limit which is $\rho_{IR} \approx 0.5$ mΩ cm with one conduction electron per Mo site. In the metals, the character of the charge transport goes through a crossoverlike change towards high temperature: the resistivity of $Nd_2Mo_2O_7$ is saturated above 500 K and the behavior of $Sm_2Mo_2O_7$ even becomes semiconductorlike above 200 K. Irrespective of the ground-state nature, the $\rho(T)$ curves tend to converge towards high temperature and the values range within a factor of 2 at $T = 600$ K. These observations suggest the hoppinglike incoherent conduction in the high-temperature state common to all the compounds and the ineffective screening of the Coulomb interaction in the whole temperature range.

We have carried out a systematic study on the evolution of the electronic structure in the broad region of the phase diagram by infrared spectroscopy. Reflectivity spectra were measured between $E = 3$ meV–6 eV below room temperature and in a slightly limited range ($E \geq 80$ meV) between $T = 300$–600 K. For the proper Kramers-Kronig analysis, the room temperature measurements were extended up to 40 eV with use of synchrotron radiation [12]. The extrapolated zero-frequency conductivity $\sigma(\omega \rightarrow 0)$ shows overall agreement with the dc resistivity data in each compound as presented in the inset of Fig. 1 for $R =$ Gd, Sm, and Nd. Some discrepancy between the temperature dependence of $\sigma(\omega \rightarrow 0)$ and σ_{dc} ($\equiv 1/\rho_{dc}$) for $Sm_2Mo_2O_7$ is perhaps due to the weak localization effect, affected by the spin-ice-like disorder of Sm moments. The wide energy-range conductivity spectra of the two edge materials are shown in the inset of Fig. 2. The Mo $4d$ intraband excitations located below $\sim$2 eV are clearly separated in case of $Nd_2Mo_2O_7$ from the higher energy O $2p \rightarrow Mo$ $4d$ charge-transfer excitations common for each compound [13].

For the study of the correlation-driven MI phenomenon we focus on the intraband transitions of the Mo $4d$ electrons. In this analysis we subtracted the contribution of the four infrared active phonon modes (observed in the range of $E = 20$–60 meV) from the raw data. The overview of the ground-state spectra is given in Fig. 2. The location of the broad maximum in the conductivity spectra of the insulators around $\hbar\omega_U \approx 1$ eV corresponds to the effective on-site Coulomb interaction, U. We determined the gap values by the linear extrapolation of the steeply increasing edge of the respective spectra as indicated in the figure. The observed Mott-Hubbard gap shows a systematic decrease with increasing r: $Ho_2Mo_2O_7$ and $Dy_2Mo_2O_7$ have a charge gap comparable to U ($\Delta \approx 250$ and 170 meV, respectively), while $Gd_2Mo_2O_7$ has almost zero gap ($\Delta \approx 20$ meV).

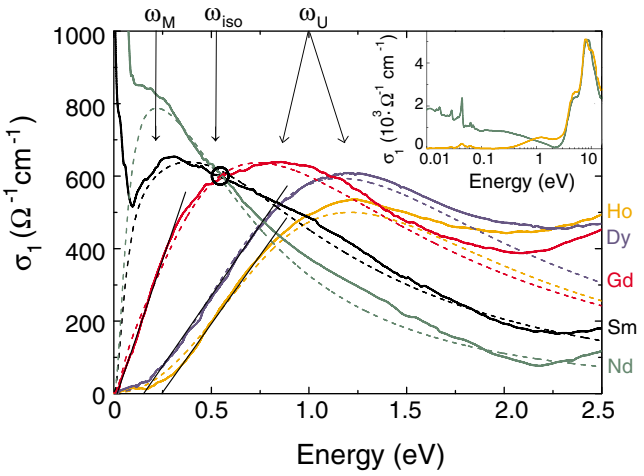

FIG. 2 (color). The $T = 10$ K spectra of the $R_2Mo_2O_7$ family. The dashed lines are the fits based on the two oscillator terms of Eq. (1). The location of the related peaks and the isosbestic point are indicated by arrows. The extrapolation to estimate the gap energy is shown by black straight lines. The broader energy-range spectra for $R =$ Ho and Nd are given in the inset. The apparent large phonon spectral intensity for $R =$ Nd is due to the electron-phonon coupling.

In going from $Gd_2Mo_2O_7$ to $Nd_2Mo_2O_7$, the recovery of the metallic character is reflected by the robust spectral weight transfer from the U peak simultaneously to a coherent part and to an incoherent midinfrared (MIR) peak centered at $\hbar\omega_M \approx 0.2$ eV. This redistribution occurs through an equal-absorption (isosbestic) point located at $\hbar\omega_{iso} \approx 0.5$ eV. Such a spectral weight transfer across the isosbestic point is a generic feature for the filling-controlled or thermally induced Mott transition [2]. The existence of an isosbestic point in the course of the present bandwidth controlled MIT can be attributed to the insignificant screening of U.

While in the spectrum of $Sm_2Mo_2O_7$ the charge-gapped feature is still discerned, the conductivity of $Nd_2Mo_2O_7$ is dominated by the Drude-like and the MIR peaks. Motivated by the presence of the equal-absorption point and the unambiguous separation of the different spectral features, we carried out a decomposition of the optical conductivity by the aforementioned three terms:

$$\sigma(\omega) = \frac{D\gamma}{\gamma^2 + \omega^2} + \sum_{i=M,U} \frac{A_i \omega^2 \Gamma_i}{\omega^2 \Gamma_i^2 + (\omega^2 - \omega_i^2)^2}. \quad (1)$$

The first is the Drude component and the two asymmetric oscillators are for fitting of the charge gap excitation and the MIR peak. The latter one is possibly related to transitions from the quasiparticle peak to the upper Hubbard band (or from the lower Hubbard band to the quasiparticle peak). The applicability of Eq. (1) to the present systems is manifested by the fact that only the weights (D, A_M, and

A_U) and the scattering rate of the coherent part (γ) have to be taken as free parameters. The related energy scales, such as the center and the width (ω_i and Γ_i, respectively) of the oscillators can be kept constant for the three (R = Nd, Sm, and Gd) compounds, irrespective of temperature. With the values of $\hbar\omega_M = 0.2$ eV, $\Gamma_M = 0.8$ eV, $\hbar\omega_U = 0.8$ eV, and $\Gamma_U = 1.8$ eV, all their spectra can be reproduced fairly well. Figures 2 and 3 show the results of the fitting for the ground-state and selected higher-temperature spectra, respectively. After the subtraction of the oscillator terms, the low-frequency part ($\hbar\omega \lesssim 0.2$ eV) is well described by the Drude form. The spectra of the insulators (R = Dy, Ho) located far from the MIT boundary is well fitted by the single term of the charge gap excitations with somewhat larger U corresponding to $\hbar\omega_U \approx 1.2$ eV.

The effective number of electrons $N_{\rm eff}$ contributing to the spectrum up to a certain energy, $\hbar\omega_c$, is defined as

$$N_{\rm eff}(\omega_c) = \frac{2m_0}{\pi e^2 N}\int_0^{\omega_c}\sigma(\omega)d\omega, \qquad (2)$$

where m_0 is the free electron mass and N is the number of Mo atoms per unit volume. After the decomposition of $\sigma(\omega)$ according to Eq. (1), the different weights are directly determined by the fits. The change in the character of the ground state is manifested in the middle panel of Fig. 4 where both the gap value (Δ) and the Drude weight ($N_{\rm eff}^D$) are plotted against r. $\Delta(r_c - r)$ decreases linearly, where the critical value $r_c \approx 1.055$ Å is close to $Gd_2Mo_2O_7$. On the metallic side, the coherent peak is built up and consequently $N_{\rm eff}^D$ emerges. The MIR peak contribution $N_{\rm eff}^M$, also plotted in the same panel, increases proportionally to $N_{\rm eff}^D$, supporting the interpretation that the MIR response is mostly due to transitions from the coherent peak to the upper band. Though there are no data in the immediate vicinity of r_c other than at the barely insulating side (R = Gd), the linear dependence of $N_{\rm eff}^D$ is suggested. In accord with the increase of $N_{\rm eff}$ below the isosbestic point, the contribution of the U peak is reduced so that the total weight is roughly conserved among the materials ($N_{\rm eff}^{\rm total} = N_{\rm eff}^D + N_{\rm eff}^{\rm MIR} + N_{\rm eff}^U = 0.38 \pm 0.06$).

Because of the proximity to the MIT point, thermal excitations radically change the electronic states in each compound. In case of the metals, the low-energy spectral weight decreases and simultaneously the role of the U peak becomes more stressful towards high temperature. At the insulating side, the effect of the elevated temperature is reversed: the priority of the U peak is suppressed by the development of low-energy incoherent excitations. These tendencies as well as the gradual loss of the coherent part can be partly discerned in Fig. 3.

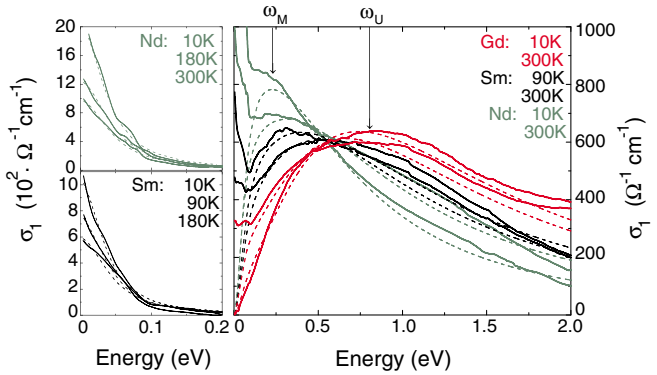

FIG. 3 (color). Right panel: the conductivity spectra of the three $R_2Mo_2O_7$ with R = Nd, Sm, and Gd, forming the isosbestic point with variations of R species and temperature. The oscillator-based fits are simultaneously plotted with dashed lines. Left panels: the low-energy spectra of the two metals after the subtraction of the oscillator terms centered at ω_M and ω_U. The dashed lines correspond to the Drude fits.

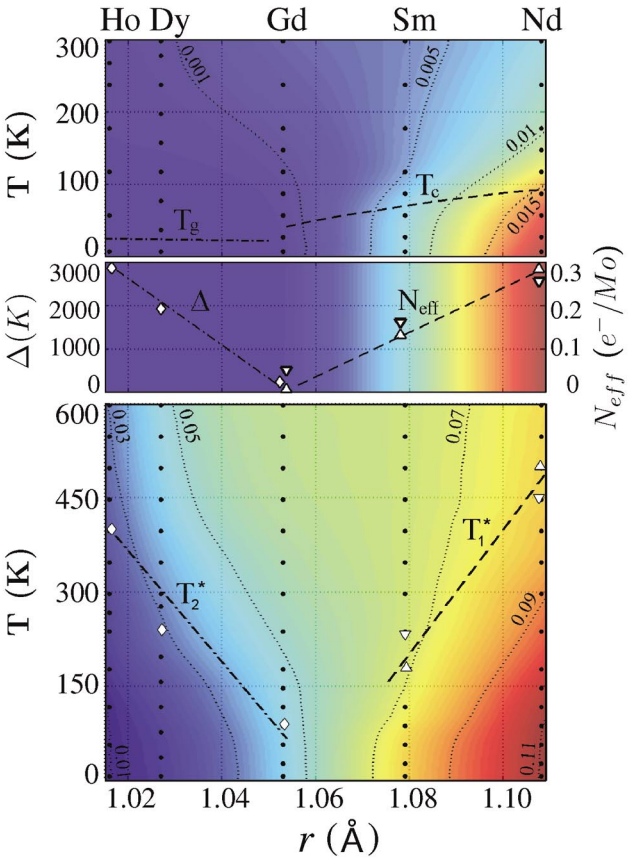

FIG. 4 (color). Linear contour map of the spectral weight on the rare-earth ionic radius (r) vs temperature plane obtained by the interpolation of the experimental data indicated by black dots. Top panel: map of the Drude weight, $N_{\rm eff}^D$. The color scaling can be checked by the numerical values on the contour lines. The magnetic phase boundaries are also indicated as showing the FM (T_c) and SG transition (T_g) temperatures. Middle panel: R dependence of the charge gap ($\diamond$), $10 \times N_{\rm eff}^D$ ($\triangle$), and $N_{\rm eff}^M$ (∇) in the ground state. $N_{\rm eff}^D(R, T = 0)$ is also represented by the color scaling which corresponds to the $T = 0$ K cross section of the top panel. Bottom panel: map of $N_{\rm eff}(\omega_{\rm iso})$, where $\omega_{\rm iso} \approx 0.5$ eV is the isosbestic point energy. Two crossover regions are indicated with T_1^* [derived both from dc ($\triangle$) and optical (∇) measurements] and T_2^* ($\diamond$).

The systematics are more clearly demonstrated in Fig. 4 by an analysis of the complete $\{r; T\}$ data set. The contour map shown in the upper panel displays the Drude weight $N_{\rm eff}^{D}(\omega_c = \gamma \approx 0.035$ eV) below room temperature. The coherence peak is preserved up to much higher temperatures than the T_c of the metallic samples and not substantially affected by the magnetic order. The coherent-incoherent crossover, where the quasiparticle peak fades and merges into the frequency independent incoherent background, occurs at $T_1^* \approx 240$ and 450 K in $Sm_2Mo_2O_7$ and $Nd_2Mo_2O_7$, respectively. T_1^* agrees fairly well with the crossover temperature observed in the resistivity curves. The mass renormalization must play a major role in the loss of the coherence since the scattering rate γ is enhanced only by $\sim$30% up to T_1^*.

We have also studied the redistribution of the spectral weight through the isosbestic point. In the light of the general relation between the effective number of electrons and the expectation value of the kinetic energy (K) that $N_{\rm eff}(\omega \rightarrow \infty) \propto \langle K \rangle$, $N_{\rm eff}(\omega_{\rm iso})$ accounts for the kinetic energy of electrons relating both to the Drude response and the MIR band (incoherent charge transport). Hence it captures the electronic-structural change relevant to the correlation-driven MIT [2,14]. Besides the temperature-induced suppression of the metallic character, the resulting contour map (the lower panel of Fig. 4) shows how the in-gap states in the insulators become gradually involved to the conduction by the thermal agitation. Though the gap is closed above T_2^* as indicated in the figure, the low-energy conductivity remains fully incoherent. This incoherent state (IS) corresponds to the plateaulike green region of the phase diagram and is characterized by hoppinglike electron transport. The IS region becomes more extended with increasing temperature and can be approached also from the metallic side through the gradual suppression of the quasiparticle weight. The uniformity of the IS is reflected not only in $N_{\rm eff}(\omega_{\rm iso})$, but the whole spectra of this region are essentially identical, irrespective of materials.

In spite of the huge temperature-induced spectral weight transfer and the distinct change of the ground state, the finite-temperature discontinuous MIT has not been observed so far in pyrochlore molybdates including also the chemically substituted compounds, $(R_x^1 R_{1-x}^2)_2 Mo_2O_7$ [5,15]. The very small charge gap of $Gd_2Mo_2O_7$ ($\Delta/U \approx 0.03$) as well as the linear dependence of $\Delta(r_c - r)$ imply that the gap closes continuously. On this basis we conclude the absence of the first-order MIT. In contrast with colossal-magnetoresistive manganites locating close to the charge-ordered-insulator–FM bicritical point [2,16], the ferromagnetism and metallicity are not so strongly coupled in pyrochlore molybdates. We found that ferromagnetism can survive beyond the MIT point. Furthermore, the magnetic ordering plays a minor role in the development of the coherent conduction. The paramagnetic phase above T_c is still metallic and the Drude weight vanishes above $T_1^* \approx 4T_c$. Though the magnetic ground state of $R_2Mo_2O_7$ is controlled by the competition between FM and AF correlations, the strong frustration reduces the temperature scale of the magnetic ordering and simultaneously suppresses the bicritical point. On the other hand, the real MIT is decoupled from the magnetic phase boundary and perhaps restricted to $T = 0$ K. The huge change in the electronic state and scattering is the consequence of the underlying zero-temperature quantum MIT.

In conclusion, we have studied the metal-insulator phenomena driven by the correlation of $4d$ electrons for pyrochlore $R_2Mo_2O_7$ single crystals by dc and optical conductivity. We identified the critical value (r_c) of the rare-earth ionic radius controlling the one-electron bandwidth, where the $T = 0$ K metal-insulator transition occurs. Approaching this point from the insulating side, the gap continuously vanishes in proportion to $(r_c - r)$, while starting from the metallic side the reduction of the Drude weight is followed. Towards high temperature the states tend to form a common incoherent conduction phase. The fundamental causes for the unique MI phenomenon are the fine tuning of the correlation strength realized in the pure (undoped) compounds and the strong frustration due to the pyrochlore lattice.

The authors are grateful to M. Imada for enlightening discussions. This work was supported in part by a Graint-In-Aid for Scientific Research, MEXT of Japan. I. K. acknowledges support from JSPS.

[1] A. Georges *et al.*, Rev. Mod. Phys. **68**, 13 (1996).
[2] M. Imada, A. Fujimori, and Y. Tokura, Rev. Mod. Phys. **70**, 1039 (1998).
[3] A. P. Mackenzie and Y. Maeno, Rev. Mod. Phys. **75**, 657 (2003).
[4] N. Ali *et al.*, J. Solid State Chem. **83**, 178 (1989).
[5] T. Katsufuji, H. Y. Hwang, and S.-W. Cheong, Phys. Rev. Lett. **84**, 1998 (2000).
[6] N. Cao *et al.*, J. Phys. Condens. Matter **7**, 2489 (1995).
[7] Y. Taguchi, K. Ohgushi, and Y. Tokura, Phys. Rev. B **65**, 115102 (2002).
[8] M. W. Kim *et al.*, Phys. Rev. Lett. **92**, 27202 (2004).
[9] J. S. Kang *et al.*, Phys. Rev. B **65**, 224422 (2002).
[10] I. V. Solovyev, Phys. Rev. B **67**, 174406 (2003).
[11] Intentional hole doping, e.g., by 5% partial substitution of Gd^{3+} with Ca^{2+}, always produces the FM ground-state irrespective of the initial metal/insulator nature of the parent $Gd_2Mo_2O_7$.
[12] For some of these materials the optical conductivity have been previously measured below $T = 300$ K by Refs. [6–8].
[13] The conductivity minimum around 2 eV becomes less pronounced toward $Ho_2Mo_2O_7$, yet still reflects the separation of the two energy scales.
[14] T. Katsufuji, Y. Okimoto, and Y. Tokura, Phys. Rev. Lett. **75**, 3497 (1995).
[15] S. Iikubo *et al.*, J. Phys. Soc. Jpn. **70**, 212 (2001).
[16] Y. Tokura, Phys. Today **56**, No. 7, 50 (2003).